Journal of Power Sources 254 (2014) 329–337

Contents lists available at ScienceDirect

Journal of Power Sources

journal homepage: www.elsevier.com/locate/jpowsour

Portable ammonia-borane-based H_2 power-pack for unmanned aerial vehicles

Jung-Eun Seo [a], Yujong Kim [a], Yongmin Kim [a], Kibeom Kim [a], Jin Hee Lee [a], Dae Hyung Lee [a,b], Yeongcheon Kim [a], Seock Jae Shin [a], Dong-Min Kim [d], Sung-Yug Kim [d], Taegyu Kim [e], Chang Won Yoon [a,b,*], Suk Woo Nam [a,b,c,*]

[a] Fuel Cell Research Center, Korea Institute of Science and Technology, Hwarangno 14-gil 5, Seongbuk-gu, Seoul 136-791, Republic of Korea
[b] Clean Energy and Chemical Engineering, University of Science and Technology, Daejeon 330-305, Republic of Korea
[c] Green School, Korea University, 145 Anam-ro, Seongbuk-gu, Seoul 136-701, Republic of Korea
[d] Korea Aerospace Research Institute, Yuseong-gu, Daejeon 305-806, Republic of Korea
[e] Department of Aerospace Engineering, Chosun University, 309 Pilmum-daero, Dong-gu, Gwangju 501-759, Republic of Korea

HIGHLIGHTS

- A portable power-pack fueled by ammonia borane (AB) was newly designed to power an unmanned aerial vehicle (UAV).
- The power-pack was demonstrated to drive a UAV for 57 min with fast load-following ability and rapid response time.
- *In situ* monitoring system was introduced to determine the filter capacity of hydrogen purification equipment.

GRAPHICAL ABSTRACT

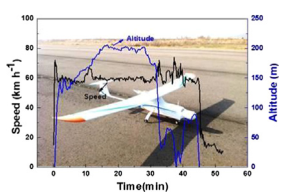

ARTICLE INFO

Article history:
Received 11 October 2013
Received in revised form
27 November 2013
Accepted 29 November 2013
Available online 27 December 2013

Keywords:
Ammonia borane
Hydrogen power-pack
Polymer electrolyte membrane fuel cell (PEMFC)
Unmanned aerial vehicle (UAV)

ABSTRACT

An advanced ammonia borane (AB)-based H_2 power-pack is designed to continually drive an unmanned aerial vehicle (UAV) for 57 min using a 200-W_e polymer electrolyte membrane fuel cell (PEMFC). In a flight test with the UAV platform integrated with the developed power-pack, pure hydrogen with an average flow rate of 3.8 $L(H_2)\ min^{-1}$ is generated by autothermal H_2-release from AB with tetraethylene glycol dimethylether (T4EGDE) as a promoter. During take-off, a hybridized power management system (PMS) consisting of the fuel cell and an auxiliary lithium-ion battery supplies 500 W_e at full power simultaneously, while the fuel cell alone provides 150–200 W_e and further recharges the auxiliary battery upon cruising. Gaseous byproducts identified by *in situ* Fourier transform infrared (FT-IR) spectroscopy during AB dehydrogenation are sequestrated using a mixed absorbent in an H_2 purification system. In addition, a real-time monitoring system is employed to determine the remaining filter capacity of the purifier at a ground control system for rapidly responding unpredictable circumstances during flight. Separate experiments are conducted to screen potential materials and methods for enhancing filter capacity in the current H_2 refining system. A prospective reactor concept for long-term fuel cell applications is proposed based on the results.

1. Introduction

Ammonia borane (NH_3BH_3, AB) is a promising hydrogen storage material that has been extensively studied as a potential fuel to replace oil for transportation applications in the last decade due to

* Corresponding authors. Fuel Cell Research Center, Korea Institute of Science and Technology, Hwarangno 14-gil 5, Seongbuk-gu, Seoul 136-791, Republic of Korea. Tel.: +82 2 958 5274; fax: +82 2 958 5199.
E-mail addresses: cwyoon@kist.re.kr (C.W. Yoon), swn@kist.re.kr (S.W. Nam).

0378-7753/$ – see front matter Crown Copyright © 2013 Published by Elsevier B.V. All rights reserved.
http://dx.doi.org/10.1016/j.jpowsour.2013.11.112

its reasonable stability under ambient conditions, high hydrogen storage capacity (19.6 wt%), and potential regenerability. The AB fuel can release hydrogen on demand via hydrolysis [1], alcoholysis [2], or thermolysis [3]. The thermally induced dehydrogenation of AB at <250 °C proved capable of enabling the generation of sufficient quantities of hydrogen with high H_2 storage density (material-based, >13 wt%). The hydrogen production via AB thermolysis is thus of particular interest for long-term applications.

For this method to be useful for desired purposes, the sluggish kinetics for AB dehydrogenation need to be improved. In this context, a number of approaches for enhancing the slow rate of AB dehydrogenation have been proposed. For example, transition-metal-based catalysts including Rh [4], Ir [5], Ru [6], Ni [7], and Fe [8] were utilized to accelerate the rates of H_2 release. Various types of chemical promoters such as proton sponge [9], ionic liquids [10,11], Lewis and Brønsted acids [12], mesoporous silica [3], diammoniate of diborane (DADB) [13], and activated boron nitride [14] were also demonstrated as efficient additives for promoting the liberation of H_2 from AB. For a continuous reactor, a liquid AB-based fuel blended with an ionic liquid (e.g., 1-butyl-3-methyl-imidazolium chloride, bmimCl) was employed for continuous hydrogen production from AB under mild conditions [10,11], which could potentially satisfy the 2015 Department of Energy (DOE) target of 5.5 wt% (system-based) for transportation applications [15]. The ionic liquids were further suggested to play a dual role as a transporting medium of AB and as a promoting additive for AB dehydrogenation [11]. Based on experimental and density functional theory (DFT) methods, a series of polyetheral promoters were suggested to enhance the reactivity of B–H bonds at AB through intermolecular hydrogen bonding interaction, which facilitated the formation of DADB, a reactive intermediate, to promote AB dehydrogenation [11,16]. Another strategy recently proposed by Varma and coworkers [17] involved a non-catalytic hydrothermal method with efficient heat management, which could produce a large quantity of hydrogen from AB with a considerably high H_2 storage capacity of ca. 14 wt% (materials-based).

Despite these accomplishments, the development of a continuous hydrogen generator utilizing AB fuel is still challenging due to the following concerns: (i) continuous supply of solid AB, (ii) purification of hydrogen containing gaseous byproducts, and (iii) discharging of liquid/solid spent-fuels from a reactor. Many studies have been conducted for the creation of an AB-based hydrogen generation system that ensures continuous feeding of AB as well as discharging of waste fuels. For example, DOE's Hydrogen Storage Engineering Center of Excellence (HSECoE) has been making significant efforts in relevant reactor design using the mixture of AB with either silicon oil [18] or ionic liquid [19]. Devarakonda et al. recently reported an auger reactor simulation using solid AB and a liquid-state AB fuel [20,21]. A novel reactor fueled by AB beads with a spinning wheel feeding system was also recently developed, which demonstrated capability to successively power a 200-W_e polymer electrolyte fuel cell (PEMFC). In this system, spherical solid AB beads were sequentially delivered into a semi-batch-type reactor filled with tetraethylene glycol dimethylether (T4EGDE), a liquid promoter [16,22]. The T4EGDE additive in the continuous reactor was suggested to play roles in (i) accelerating the H_2-release kinetics, (ii) suppressing the formation of scatters/impurities and foaming upon dehydrogenation, and (iii) fluidizing solid spent-fuels [23]. For practical applications, an improved reactor concept was proposed by introducing H_2 purification equipment with high filter capacity and an efficient drainage system for spent fuels.

We report here on a portable hydrogen power-pack fueled by solid AB pellets, which mainly comprises an AB-based hydrogen generator, a hybridized power management system (PMS) installed with a 200-W_e PEMFC, an auxiliary battery, and a control unit. The performance of the developed hydrogen power-pack was then assessed by integration into an unmanned aerial vehicle (UAV) platform under collaboration with the Korea Aerospace Research Institute (KARI). To the best of our knowledge, no continuous AB-based H_2 generator has previously been applied for a practical application to date. The ability of the power-pack to continuously drive a UAV for 57 min with fast load-following ability and rapid response time was verified. The fuel cell with the AB-based H_2 production system was found to provide supplemental power to recharge the auxiliary battery during operation. Plausible strategies for enhancing the efficiency of the hydrogen generator are discussed based on additional experiments.

2. Experimental setup

2.1. Materials

The AB solids (Aviabor, 98%) were pulverized into fine powers by a commercial grinder under N_2 atmosphere, followed by pelletizing into spherical beads using a manual dry pressing process [23]. The AB beads weighed ca. 0.082 g, with a diameter of 5.7 mm, and density of ca. 0.74 g cm^{-3}. Supposing that one AB bead releases 2 equiv. of H_2, the AB pellet can produce ca. 130 mL of H_2. Tetraethylene glycol dimethylether (T4EGDE, Sigma Aldrich, 99%) and triethylene glycol dimethylether (T3EGDE, Sigma Aldrich, 99%) were employed without further purification and stored under an atmosphere of N_2 at room temperature.

2.2. Procedure for hydrogen production with the developed H_2 generator

An AB-powered continuous H_2 generator with fast dehydrogenation rates up to 3.3 L(H_2) min^{-1} and fast load-following capability was recently constructed [23]. Providing a continuous supply of the AB/T4EGDE mixtures (AB:T4EGDE = 50:50, wt%) in a liquid phase was found to be difficult due to the limited AB solubility towards T4EGDE. In addition, since the T4EGDE promoter was exuded upon pelletizing the mixtures of AB and T4EGDE, the delivery of the AB/T4EGDE mixtures in a solid state was unsuccessful. For these reasons, desired amounts of the liquid T4EGDE promoter (120 g) were pre-loaded in a semi-batch-type reactor while solid AB pellets (with a stored weight of 110 g) were supplied into the reactor by adjusting feeding rates in the range of 2.46–2.54 g min^{-1}. The AB contents (relative to AB + T4EGDE) in the reactor thus varied from 0.0 to a maximum of 48 wt% as a function of time. The AB powders were pelletized into a spherical form, and one AB bead had an average weight of 0.082 g (Fig S1), which could theoretically produce ca. 130 mL(H_2) upon releasing 2 equiv. of H_2. Continuous supply of the AB beads into a semi-batch-type reactor was achieved using a spinning-wheel-type conveyer.

2.3. Configuration of the developed fuel cell system for a UAV

The fuel cell power-pack utilizing both AB beads and T4EGDE consisted of (i) a continuous hydrogen generator, (ii) a hybridized power management system (PMS) equipped with a commercial 200-W_e PEMFC stack (AEROPAK [24]) as well as an auxiliary lithium-ion battery (Kokam), and (iii) control panels, as depicted in Fig. 1a. The developed H_2 generator was also composed of (1) a storage tank for the AB beads, (2) a conveying system, (3) a semi-batch reactor, and (4) an external H_2 purification system (Fig. 1b, red box). This H_2 production system has different features from the previous H_2 generator, in that (i) The dimensions of the fuel tank for the AB beads were expanded to increase the maximum storage from 80 g (1000 ea.) [23] to 120 g (ca. 1500 ea.) of AB, (ii) a worm-

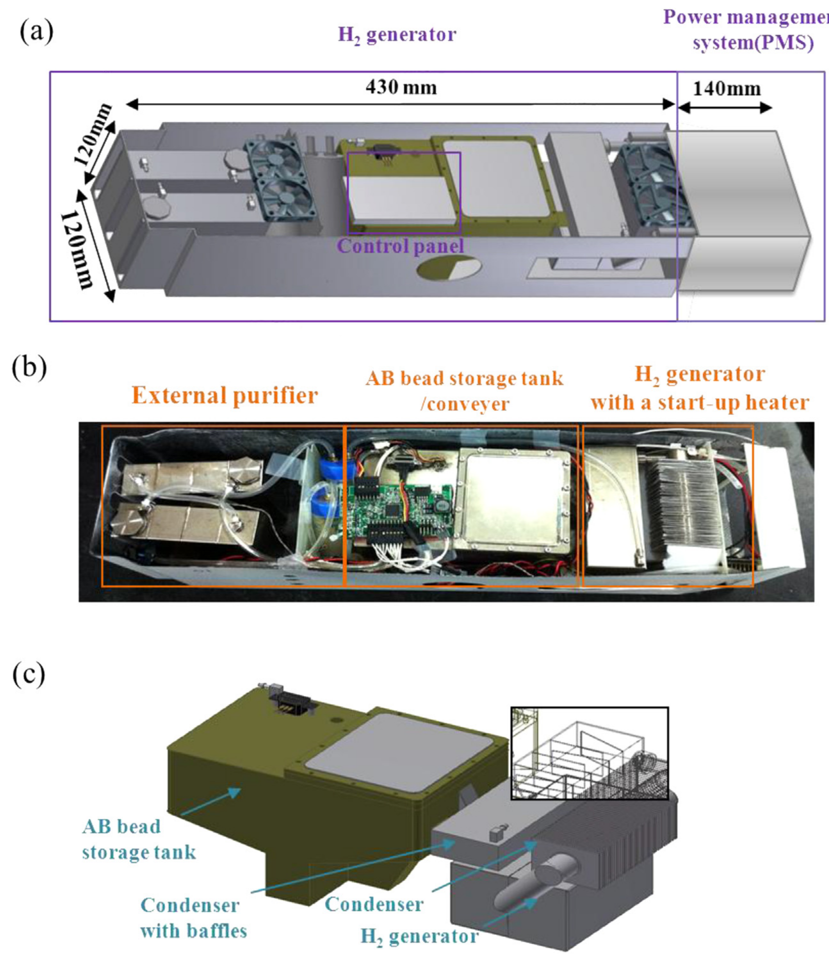

Fig. 1. The AB-based hydrogen generator: (a) 3-D sketch, (b) completely integrated AB-based H_2 generator, and (c) the detailed 3-D sketch of the subpart including AB bead storage tank, H_2 generator, and two condensers.

geared BLDC motor (NIDEC 13H220E011; speed: 6200 rpm; current: 0.15 A; voltage: 12 V) was employed to enhance the stability of the current spinning wheel system, (iii) the filter capacity of a H_2 purification system was improved by using mixed carbon-based absorbents with cooling fans, (iv) a condenser with baffles was installed to provide an elongated pathway for facile separation of effluents from evaporated T4EGDE molecules, and (v) a relief valve was used to maintain the internal pressure of the reactor with a maximum pressure of 150 kPa.

2.4. Integration of a UAV and a flight test

To evaluate the performance of the developed fuel cell system integrated with an AB-based H_2 generator [25], this system was applied to a UAV (Ucon System, RemoEye-006) that includes a platform, sensors, data links, and ground control stations. The detailed specifications are listed in Table 1. The UAV can be utilized for reconnaissance, and has clear limitations in the dimensions and weight for the targeted H_2 generator. In general, the dimensions and weight of a UAV platform must be minimized to maximize flight time with high efficiency. The dimensions of the space for the AB-based hydrogen generator in the UAV fuselage was limited to 610 mm × 120 mm × 120 mm. The permissible weight for the fuel cell system including the AB-based H_2 generator and 200-W_e PEMFC stack is limited to 2800 g in the UAV platform. Since the weight of the commercial stack (AEROPAK [24]) is 470 g, the total weight of the H_2 generation system including AB pellets, T4EGDE, and filter materials should be lower than 2330 g. The AB-based H_2 generator was designed to have a weight of 1706 g. In addition, the weights of AB beads and the T4EGDE promoter were limited to 110 g and 120 g, respectively. 260 g activated carbon materials (3M 6001, 6006) were employed as filtering absorbents to remove undesired byproducts. The detailed weight distribution of the fuel cell system is listed in Table 2.

Table 1
Specification of the UAV platform.

Item	Value
Wing span	2.9 m
Length overall	1.8 m
Max launching weight	7.5 kg
Payload	0.3 kg
Wing area (S)	0.7515 m^2
Aspect ratio (AR)	10.0
Max level speed	75 kph
Operation range	15 km
Endurance with Li-polymer-battery-type power source	1.5 h
Propulsion	Electric motor
Aviation type	Glider type
Materials	Carbon/glass hybrid fibers Carbon tube
Motor type and power	Brushless DC 900 W (maximum output)

Since a UAV requires a large power range and a fast response during take-off, cruising, maneuvering, and landing, an efficient power management system (PMS) is required to respond to unpredicted circumstances. For example, a platform needs an immense amount of power within an instant period of time during take-off. In the present PMS, a fuel cell and an auxiliary battery were hybridized in parallel. The commercial battery employed in this study has 70 × 34 × 22 mm in size with a weight of 119 g. The capacity and voltage of the battery are 1300 mAh and 11.1 V, respectively. Two batteries were employed following connection in series. If the UAV platform is operated with only the fully charged auxiliary battery (28.8 Wh), the flight time will be limited to ca. 8 min. The role of the lithium-polymer battery in the PMS is to supply power upon a sudden increase of load and for emergency landings. Since the electric motor required a total power of 500 W_e for take-off, both the battery and fuel cell were simultaneously employed to supply a combined power of 500 W_e. During cruising and maneuvering, the fuel cell provided a sufficient power of 180–200 W_e and also recharged the battery. This fuel cell system was integrated into the UAV test platform, and flight tests were conducted at the Goheung Aviation Center at the Korea Aerospace Research Institute.

2.5. Characterization of effluents produced from the H_2 generator

Quantitative and qualitative analyses of gaseous byproducts during the dehydrogenation of the AB beads with T4EGDE were initially performed *in situ* using a customized gas cell positioned in an FT-IR spectrometer (Nicolet iS10, Thermo Scientific) equipped with an MCT detector and an FT-IR spectrometer (FTIR-7600, Lambda) with a DTGS detector. Spectral data were collected using a scan rate of 8 scans cm^{-1} with a resolution of 4 cm^{-1}. Gram–Schmidt curves obtained by a Nicolet FT-IR spectrometer provided relative quantities of gases as a function of time, with a higher intensity indicating the formation of more gaseous byproducts. In conjunction with the FT-IR spectroscopic studies, the gaseous byproducts trapped in T4EGDE (5 mL) were further analyzed using a 600-MHz FT-NMR spectrometer (Varian) calibrated with BF_3OEt_2 ($\delta = 0.0$ ppm) as an external reference.

2.6. Determination of the filter capacities

In a separate experiment, a reactor equipped with T4EGDE (25 g) was initially soaked in a silicon oil bath pre-heated at 120 °C, and the AB pellets were then supplied into the reactor with a feeding rate of 0.18 g min^{-1}. Under these conditions, the rate of hydrogen production was expected to be 0.28 L(H_2) min^{-1}. The gaseous byproducts produced from the mixture of AB and T4EGDE were then delivered into a purification system initially utilizing a number of solid materials including commercial activated carbon filters (3M): (1) 3M 6006, (2) 3M 6004, (3) 3M 6001, (4) 3M (6001 + 6006), (5) a Metal-organic-framework (MOF), (6) a mixture of 3M 6006 and silica gel (Sigma Aldrich, Grade 12, 28–200 mesh), (7) carbon paper, (8) grinded 3M 6006 (pulverized activated carbon with average particle sizes of 0.3 mm), (9) a mixture of 3M 6001 and 6006 with cooling, and (10) a mixture of pre-dried 3M 6001 and 6006 with cooling. In the case of the utilization of the T4EGDE trap, the produced gases were designed to be bubbled through a pipe with an inner diameter of either 1.6 mm or 0.6 mm (Fig. S2). The carbon trap was filled with 5 g of the mixture of 3M 6001 and 6006 (50:50, wt%), and changes in temperatures at three different points (T1, T2, and T3) were monitored using an electric temperature controller (Hanyoung, NX4). The temperatures T1, T2, and T3 determined the temperatures of gases, the gas–absorbent interface, and the absorbents, respectively (Fig. S2). The effluents following the sequestration of the produced gaseous molecules were further monitored *in situ* by an FT-IR spectrometer.

The UAV platform employed only the mixtures of activated carbon-based absorbents (3M 6001 and 6006) to remove undesired byproducts. To monitor the filter capacity as a function of time during flight, the temperatures at three different points (Fig. S3) were also measured: (i) at the exterior of the reactor (T1), (ii) the exterior of the reactor (T2), and (iii) the middle of the filter materials (T3). The filter capacity (FC) was calculated using the following formula: FC ($g_{AB}\ g_{trap}^{-1}$) = weight of ammonia borane used/weight of filter employed. A filter capacity of 1 $g_{AB}\ g_{trap}^{-1}$ indicates that 1 g of the filter material can sequester gas byproducts produced from 1 g of AB upon thermolysis.

Table 2
Weight distribution of the H_2 power-pack.

Item		Weight (g)
200 W_e fuel cell stack		470
H_2 generation system	Case	348
	Start-up heater	225
	Reactor	436
	Feeder	166
	Electron wire	133
	Board	41
	Recycling pump	53
	Press pump	55
	Filter case	203
	Paper filter	46
	Total	1706
Filter materials		260
Fuel (AB beads)		110
Promoter (T4EGDE)		120
Total		2666

3. Results and discussion

3.1. Integration of an improved AB-based hydrogen generator

Sneddon and coworkers demonstrated thermally induced dehydrogenation from a mixture of AB and T4EGDE (50:50, wt%) at 85 °C as an efficient method for hydrogen production [26]. Likewise, H_2-release properties were recently shown with mixtures of AB and a series of polyethers ($CH_3O-(CH_2CH_2)_n-OCH_3$, $n = 1$–4) with a weight ratio of AB:polyether = 70:30 at >85 °C. In addition, based on both experiments and DFT calculations, it was proposed that electron transfer from a polyether into AB via hydrogen bonding interaction could increase the hydricity of B–H at AB, ultimately enhancing the rate of H_2-release from AB [16]. Notably, the dehydrogenation kinetics was retarded at extremely low AB content (<5 wt% with respect to AB + polyether) presumably because the excess of a polyether hindered intermolecular interaction between ABs [16]. An AB-based hydrogen generator was developed utilizing T4EGDE to demonstrate its capability to continuously generate H_2, powering a 200-W_e PEMFC stack for 25 min [23]. This H_2 generator was operated autothermally without an external heater by recycling waste heat produced during AB dehydrogenation. Upon AB feeding with a rate of 2.2 g min^{-1}, the H_2 production system released H_2 with a rate of 3.3 L min^{-1} along with a heat of 44 W, which increased the reactor temperature from 120 °C to 160 °C. The increased temperature of >145 °C, however, could cause the formation of significant quantities of gases (e.g., borazine, $B_3N_3H_6$) that are detrimental to a PEMFC stack, thus requiring increased amounts of filter materials. In addition, substantial quantities of cross-linked byproducts such as polyaminoborane (PAB), polyiminoborane (PIB), and polyborazylene would be formed as

liquid/solid spent-fuels at high temperatures [27], which may lead to significant problems upon discharging the spent-fuels. To apply this previously developed AB-based power pack for long-term applications, the filter capacity needs to be maximized along with enhancement of the fluidity of the spent-fuels.

Building upon the issues raised in previous studies, the performance of the former AB-based continuous H_2 generator was improved for practical applications, primarily by (i) reducing the weight of a semi-batch-type H_2 generator equipped with a start-up heater for the heat generation of 80 W, (ii) increasing the storage capacity of an AB bead tank, and (iii) enhancing the capacity of an external purifier using two different types of commercial 3M absorbents, as depicted in Fig. 1. In addition, two condensers with baffles were further introduced to separate gases (H_2 + other gaseous byproducts) with vaporized T4EGDE, which helped prevent clogging inside the narrow gas tube potentially induced by byproducts condensation (Fig. 1c). By addressing these issues, an advanced AB-based H_2 generator was created using T4EGDE as a promoter that was further integrated with a 200-W_e PEMFC stack. The capability of the resulting power-pack to power an UAV was then demonstrated.

3.2. Development of a lightweight PEMFC stack

To achieve a power-pack system fueled by alternative chemical fuels (e.g., AB) for portable applications, a viable fuel cell system needs to be developed along with a H_2 generator. In this context, a lightweight PEMFC stack was also developed to take the maximum take-off weight into consideration. In order to reduce the stack weight, metal sheets were formed into meandering bipolar plates, and honeycomb composites were fabricated as end-plates. A membrane electrode assembly (MEA) was prepared by coating 0.3 mg cm^{-2} of Pt/C on both sides of a polymer electrolyte membrane (Nafion-112) using a programmable auto-spray coater. Carbon paper (TGP-H-090, 260 μm) was used as a gas diffusion layer (GDL). The border of MEAs was then sealed by Teflon glue. The developed stack featured an air-breathing open-cathode and dead-ended anode operation. The single cell including MEA and bipolar plate has 42.5 × 75.5 × 2.64 mm in size. The active area of a single cell was determined to 31.5 cm^2. 35 cells were stacked to generate the desired power output of 200 W_e. The weight of the fabricated stack was 380 g, and after being assembled with other components including an air-fan, anode purging valve, controller, and housing (Fig. 2), it weighed 430 g. The stack controller was programmed to control the air-fan and purging valve. The speed of the air-fan was controlled according to the stack temperature, and the purging valve was opened and closed periodically to prevent water flooding. The power density of the PEMFC stack was 463 W kg^{-1}, which is high enough for use as a power source in the UAV.

Fig. 3 shows the *I*–*V* performance curve of the developed PEMFC stack. High-purity hydrogen gas was used, with the supply pressure being fixed at 150 kPa. The power load was controlled by an electronic load device. The voltage, current, temperatures, and hydrogen flow rate were recorded by a DAQ board and monitored in LabView software. The capability of this fully assembled stack including the air-fan, valve, controller, and housing was examined in a ground test, which indicated that the rated power output was 210 W at an electric load of 10 A and stack voltage of 21 V. The observed high performance, however, was found to decrease particularly at low temperatures. To evaluate the feasibility of the developed AB-based H_2 generator as an efficient power source for a practical application, the commercial stack was installed into the developed H_2 generator and employed to obtain reproducible data for flight tests.

3.3. Integration of fuel cell power-pack into the UAV and flight tests

To evaluate the performance of the fuel cell power-pack, this system was integrated into a UAV platform and ground and flight tests were performed. Following the installation of the AB-based power pack into a UAV (Fig. 4a), the assembled UAV (Fig. 4b) was initially operated manually under a continuous power consumption of 200 W_e in ground tests to examine the capability of H_2 production as a function of time. The UAV was then launched using both the battery and the fuel cell, and its flight motion was controlled manually by a pilot. During cruising, flight data were automatically collected at a ground control system through RF communication with the UAV. The results of the flight test including flight trajectories, aircraft movement (angles of roll and pitch), altitudes, and speeds of the aircraft are summarized in Fig. 5. The aircraft trajectory mainly reflected a circular shape with a radius of approximately 500 m with respect to the ground control system (Fig. 5a). The roll and pitch angles recorded during flight were in the range of −30° to 20° and −5° to 10°, respectively (Fig. 5b), suggesting that the AB-based power pack can be applied as a power source in various types of aircrafts under normal flight conditions. The UAV was mainly maneuvered at an altitude of 200 m with a cruising speed of 60 km h^{-1} (Fig. 5c). In this flight test, the AB pellets were found to be continuously supplied into the reactor with a feeding rate of ca. 2.5 g min^{-1} (30 ea. min^{-1}) for a

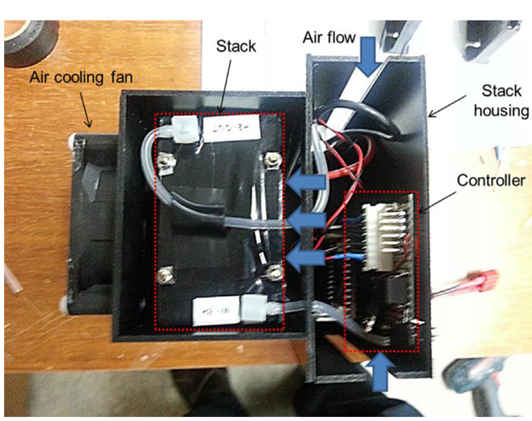

Fig. 2. The assembled PEMFC stack.

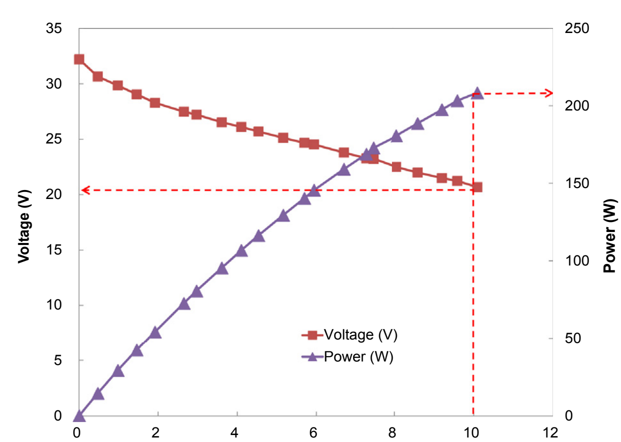

Fig. 3. *I*–*V* performance curve of the developed PEMFC stack.

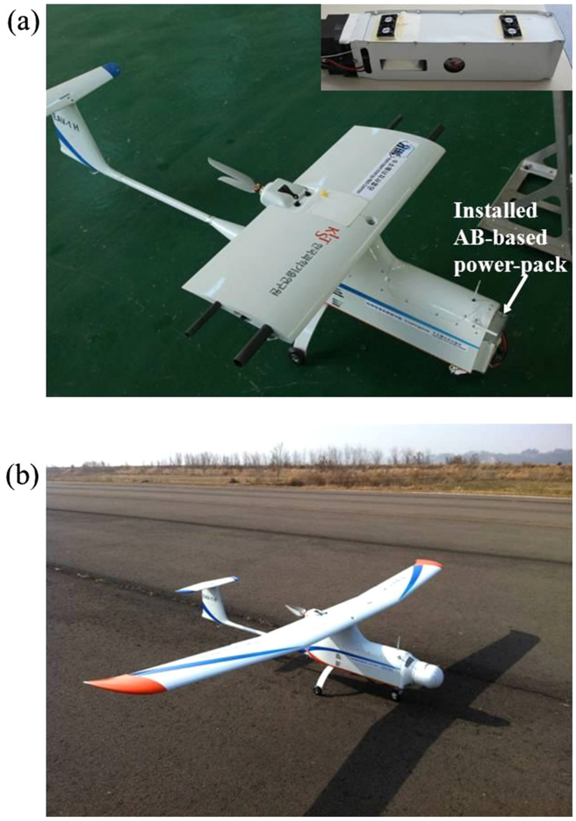

Fig. 4. The UAV platform: (a) installation of the as-developed power pack into the UAV and the AB power pack (inset) and (b) the fully-assembled UAV before the test flight.

total feeding time of 57 min. The inlet pressure of the PEMFC stack was sustained at 150 kPa during the early stages of the flight, and for pressure higher than 150 kPa, a pressure relief valve was designed to function. The inlet pressures of the stack showed a bit of fluctuation as a function of time, presumably because the condensation of gaseous byproducts (e.g., borazine, b.p. 53 °C at 100 kPa) induced by cold atmosphere (ca. 4 °C at ground) led to clogging of the pipelines connected to the pressure relief valve. In order to prevent this problem, the current pipelines need to be replaced by pipelines with an increased diameter. Enhanced filter capacity for byproduct sequestration could also suppress the clogging issue. Note that the rate of hydrogen production (3.8 L min^{-1}) was always faster than that of hydrogen consumption (ca. 2.8 L min^{-1}) in the PEMFC stack, which indicates that the considerable amounts of H_2 unconsumed by the PEMFC stack were exhausted outward, reducing the flight time (<1 h) (Fig. 5c). The flight time can thus be increased by adjusting the AB feeding rate according to the power consumption.

The evolution of power generated from the fuel cell stack and the auxiliary battery is illustrated in Fig. 6. During take-off, the electric motor abruptly consumed ca. 500 W_e to drive the propeller of the UAV platform. This power was supplied by both the auxiliary battery and the fuel cell. During cruising and maneuvering, however, power ranging from 150 to 200 W_e within 30 min was mainly supplied from the fuel cell stack. This clearly indicates that the developed AB-based power pack continuously generated hydrogen to operate the UAV platform without failure. To examine the capability of the hybridized PMS under different circumstances, the UAV was maneuvered by adjusting the pitch and roll angles and the altitudes between 30 min and 45 min (Fig. 5b), which afforded significant fluctuation of the power consumption (Fig. 6). It is evident that the fuel cell and battery in the hybridized PMS were synchronized to provide stable power for cruising and maneuvering even under these severe circumstances. When the fuel cell power decreased, the battery power increased, and vice versa.

3.4. Hydrogen purification system

The AB dehydrogenation reactions with T4EGDE conducted at an initial temperature of >120 °C could likely produce gaseous spent fuels containing B=N bonds (e.g., borazine, $B_3N_3H_6$) as well as ammonia, along with >2 equiv. of H_2. *In situ* FT-IR spectroscopy confirmed the formation of ammonia (920 cm^{-1}), μ-aminodiborane (1558, 2409, 2589, and 3481 cm^{-1}), and borazine (1459, 2526, and 3481 cm^{-1}) during the H_2-release from the mixture of AB and T4EGDE at 120 °C, and the quantities of these byproducts increased with time (Fig. 7a, [16]). These byproducts were then trapped in T4EGDE at 25 °C, followed by additional characterization using ^{11}B NMR spectroscopy. Consistent with the results obtained by the FT-

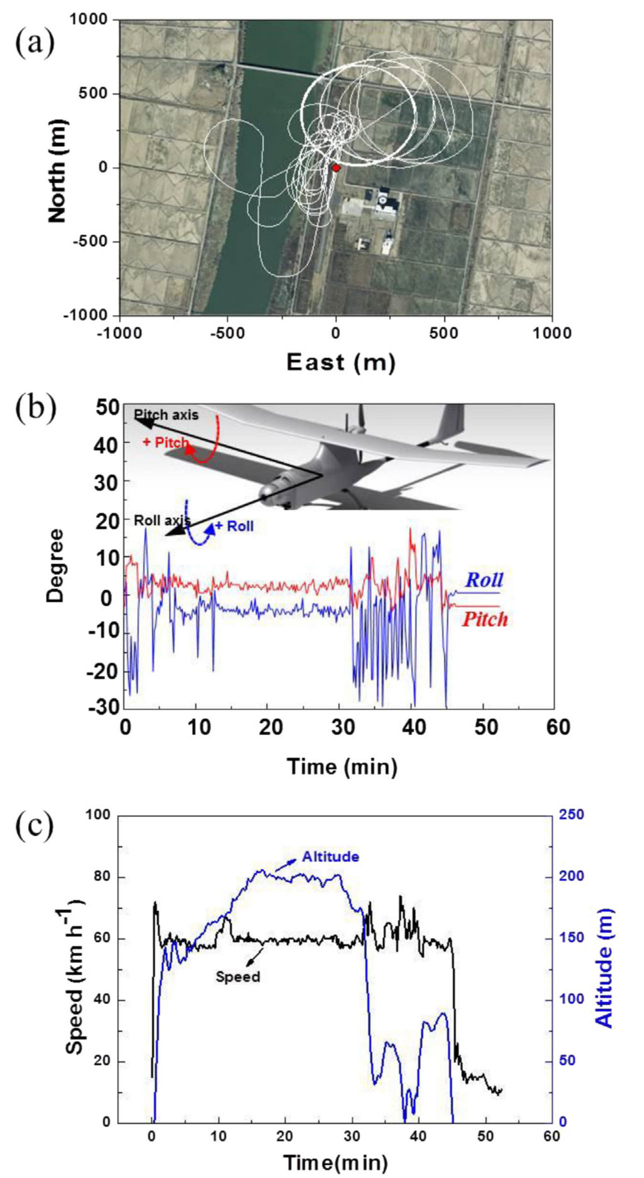

Fig. 5. Results for a flight test: (a) aircraft trajectory (the red diamond symbol represents the position of the ground control system; white line represents trajectory of the UAV), (b) the evolution of the flight attitude (roll and pitch), and (c) the evolution of flight speed and altitude. (For interpretation of the references to color in this figure legend, the reader is referred to the web version of this article.)

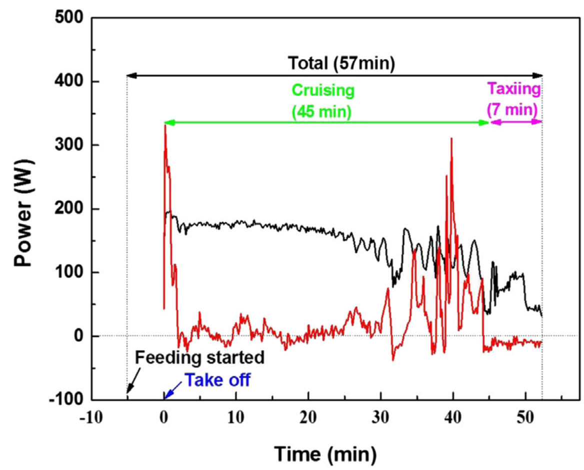

Fig. 6. The evolution of power generated from the fuel cell stack and the auxiliary battery (black line, fuel cell; red line, auxiliary battery). (For interpretation of the references to color in this figure legend, the reader is referred to the web version of this article.)

IR spectroscopic studies, ^{11}B NMR spectroscopy indicated that the signals centered at $\delta = -27$ ppm as well as at $\delta = 31$ ppm were attributed to the formation of μ-aminodiborane and borazine, respectively (Fig. 7b). These results are in line with the previous reports regarding AB dehydrogenation with T4EGDE [16] or with T3EGDE (triethylene glycol dimethylether) [28]. Since these gaseous spent fuels likely poison the Pt catalysts in a PEMFC [29], they should be sequestrated by a purification system in the platform. The determination of a usable filter capacity of the purifier as a function of time would thus provide valuable information. For example, when the filter capacity measured at a ground control center reaches close to its maximum value, then action can be taken (e.g., manual landing).

In this context, a real-time monitoring system that can determine the remaining filter capacity of the purification system at a ground control center was introduced. In separate experiments, AB dehydrogenation reactions with T4EGDE at 120 °C were conducted in a batch reactor, and prior to the detection of byproduct gases using FT-IR spectroscopy, they were delivered into a trap filled with various kinds of solid materials. Upon sequestration of the gaseous byproducts at the surface of the filter materials, additional heat was found to be released, presumably due to the exothermic nature of chemical reactions between carbon-based filter materials and gaseous spent-fuels. The real-time monitoring system essentially detected the produced heat, thus measuring the temperatures of the purifier *in situ* at three different points (top, T1; middle, T2; bottom, T3; Fig. S2). Note that T1, T2, and T3 determined the temperatures of gases, the interface of gases-solid filter material, and solid filter material, respectively. The temperature profiles shown in Fig. 8 indicate that the temperature of gaseous byproducts (T1) kept constant while T2 and T3 varied with time. The T2

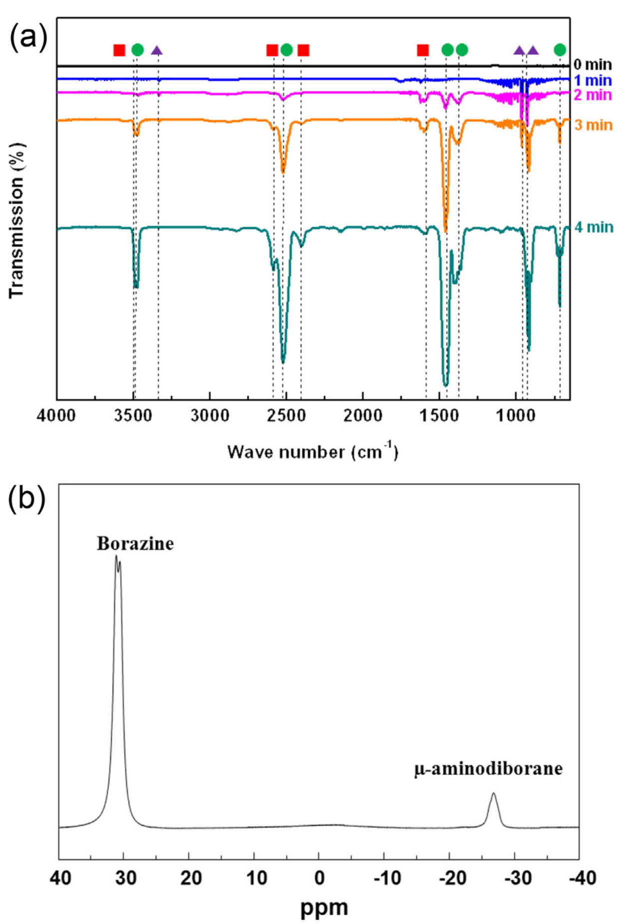

Fig. 7. Characterization of byproducts: (a) *in situ* FT-IR spectra of the gaseous byproducts produced during T4EGDE-mediated thermolyses and (b) ^{11}B NMR spectrum of the gaseous byproducts trapped in T4EGDE.

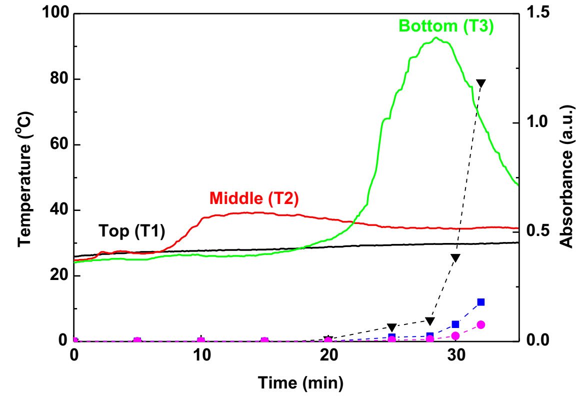

Fig. 8. Temperature profiles of the filter system (3M 6006) measured at three different points (T1, T2, and T3, respectively). The details of filter system were depicted in Fig. S2. The FT-IR intensities of the produced borazine (▼, 1459 cm^{-1}), μ-aminoborane (◆, 2589 cm^{-1}), and ammonia (■, 920 cm^{-1}) were also shown (*Y* axis in the right side).

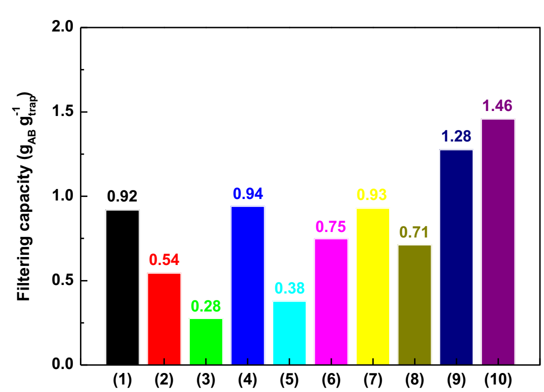

Fig. 9. Screening results for hydrogen purification methods based on FT-IR analyses of the release gases during T4EGDE-mediated thermolyses of AB at 120 °C with different filtration methods. AB = 0.18 g min^{-1}, T4EGDE = 25 g: (1) 3M 6006, (2) 3M 6004, (3) 3M 6001, (4) 3M (6001 + 6006), (5) a MOF, (6) 3M 6006 + silica gel, (7) carbon paper, (8) grinded 3M 6006, (9) 3M (6001 + 6006) + cooling, and (10) pre-dried 3M (6001 + 6006) + cooling.

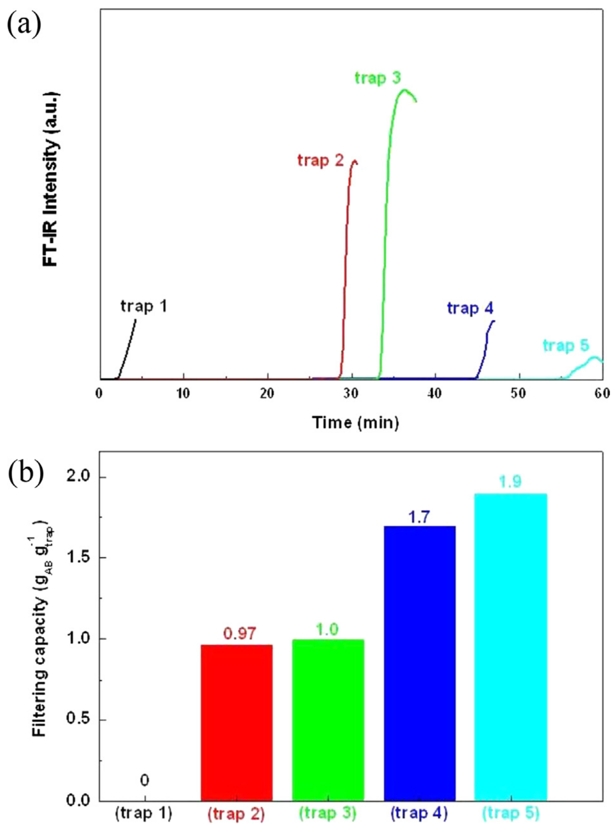

Fig. 10. Screening results for hydrogen purification methods: (a) FT-IR analyses of the release gases during T4EGDE-mediated thermolyses of AB at 120 °C with or without different filtration methods. AB = 0.18 g min^{-1}, T4EGDE = 25 g, Starting temperature = 120 °C, and (b) the determined filter capacities.

temperature increased slightly after 12 min to reach a maximum of 40 °C and was maintained until ca. 20 min. Considering that the process of byproduct removal was exothermic but the produced heat was radiated spatially, this result is presumably due to the thermal equilibrium at the interface between gases and solid absorbents. The temperature (T2) then decreased slightly after 20 min simultaneously along with rapidly increasing the T3 temperature. When the undesired gases were successively penetrated into the filter, the absorbent located at the bottom began to be deactivated, ultimately exceeding its filter capacity. Consistent with this explanation, the FT-IR spectroscopy revealed that the unremoved borazine, μ-aminodiborane, and ammonia appeared at 25 min (Fig. 8). The filter materials were also found to release tiny amounts of carbon dioxide and water. Following initial heat treatment of the carbon-based materials at 120 °C for 2–3 h under dynamic vacuum, reduced quantities of the byproducts, CO_2, and H_2O were released, suggesting that the produced CO_2 and H_2O molecules may be attributed to physisorbed species. Other solid filter materials were further screened, and it was found that the combination of 3M 6001 and 6006 possessed higher filter capacity than other solid materials, as summarized in Fig. 9.

In this flight test, based on the experimental results describe above, an external purification system containing mixed, activated carbons (3M 6001 and 6006) was employed and further demonstrated to remove the produced borazine, μ-aminodiborane, and ammonia, which allowed the UAV platform to operate for 57 min. For a long-term UAV application with high efficiency, however, the purification capacity of the filter system in the developed hydrogen generator needs to be improved. An *in situ* monitoring system was employed to screen efficient methods for improving the filter capacity of activated carbon. Since the produced boron containing byproducts can readily be hydrolyzed by acid, the filter material (a heterogeneous mixture of 3M 6001 and 6006) was initially treated with sulfuric acid (8.9 M) for 12 h at 80 °C, followed by evaluation of its filter capacity using FT-IR spectroscopy. No trap (trap **1**) was also employed for comparison. Compared to the original carbon-based materials (trap **2**), the acid-treated activated carbon (trap **3**) showed an increased filter capacity by 3%, as evidenced by the delayed appearance of borazine from 32 min to 33 min (Fig. 10a). T4EGDE was further considered as a potential filtering agent, with an assumption that the liquid T4EGDE promoter used for AB dehydrogenation can be recycled. To validate this hypothesis, the capacities of combined filter systems using T4EGDE were examined (traps **4** and **5**, Fig. S2). Compared to the capacity of trap **2**, they were significantly increased (Fig. 10a). For example, more than 75%

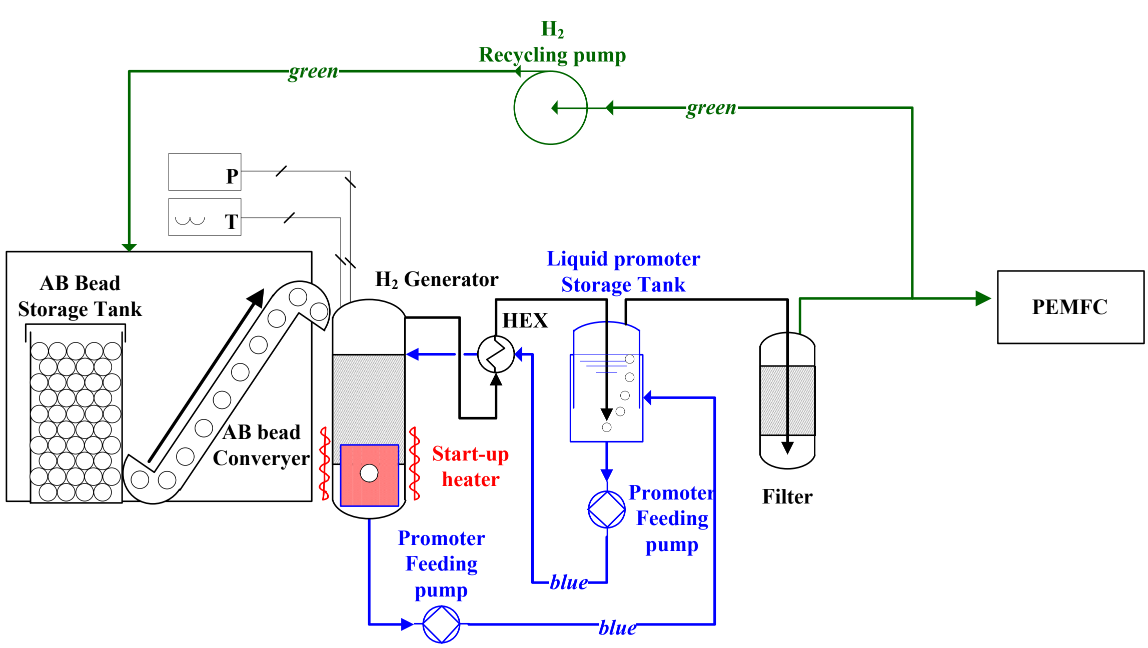

Fig. 11. The proposed fuel cell system powered by AB for the prolonged operation.

of the gaseous byproducts were sequestrated using activated carbon, followed by the T4EGDE trap that possessed a glass pipe with an inner radius of 1.6 mm (trap **4**). Notably, upon utilization of a glass pipe with an inner radius of 0.6 mm for the T4EGDE system (trap **5**), this capacity was found to be further enhanced by 96% with respect to trap **2**, which was employed in the UAV platform. The calculated filter capacities of the traps described above are compared in Fig. 10b. These results strongly suggest that the weight of the platform can be reduced by developing an improved purification system using T4EGDE.

4. Conclusions

A novel AB-based H_2 generator has been created, and its ability to continuously operate a PEMFC at a rated power of 200 W_e was demonstrated for an UAV application. In this system, the T4EGDE-mediated AB dehydrogenation was employed to achieve the targeted flow rate of 3.3 $L(H_2)\ min^{-1}$, and the waste heat produced during AB hydrogenation was recycled for the autothermal operation of the UAV platform. The total duration time for H_2 production including the processes for pre-heating, take-off, cruising and maneuvering, and taxiing was close to 1 h. In addition, a real-time monitoring system for the determination of the remaining filter capacity was introduced and applied to the platform. Based on this *in situ* monitoring procedure, other potential methods for enhancing the filter capacity of the purification system were screened. It was demonstrated that the use of T4EGDE as an additional trap along with the activated carbon materials particularly increased the sequestration capability of the H_2 purification system.

Based on the results, an advanced reactor concept for long-term applications has been suggested, as shown in Fig. 11. In this concept, a storage tank for the liquid promoter is positioned separately from the reactor and continuously supplies T4EGDE. In parallel, the AB pellets are fed from the AB storage tank. The gaseous byproducts produced may initially be bubbling through the T4EGDE tank, followed by removal at a physical trap filled with a mixture of activated carbon, according to the preliminary results shown in Fig. 10. To prevent backflow of the partially vaporized liquid promoter (e.g., T4EGDE) and gaseous byproducts from the reactor during dehydrogenation, parts of the purified hydrogen may be recycled into the AB storage tank [23]. As a result, a lightweight H_2 generator with high filter capacity can be realized for long-term applications.

Optimization for the discharging of liquid/solid spent fuels is still necessary. In general, waste fuels were solidified as dehydrogenation proceeded, which could not only influence the rates of H_2 release, but also cause potential clogging problems upon ventilation of the spent fuels. It was recently found that T3EGDE (triethylene glycol dimethylether) could enhance the fluidity of the liquid/solid spent fuels produced during dehydrogenation, and further studies are being conducted to resolve this issue. With these strategies, an improved fuel cell system with high specific energy could be achieved, and could be further applied to a number of medium or large-scale applications.

Acknowledgments

This research was supported by Korea Institute of Energy Technology Evaluation and Planning (KETEP) of the Ministry of Knowledge Economy (MEST) (the New Renewable Energy Program, NO. 20113030040020). Part of this research was also supported by the National Research Foundation of Korea Grant funded by the Korean Government (MSIP) (2013, University-Institute cooperation program).

Appendix A. Supplementary data

Supplementary data related to this article can be found at http://dx.doi.org/10.1016/j.jpowsour.2013.11.112.

References

[1] M. Chandra, Q. Xu, J. Power Sources 156 (2006) 190–194.
[2] P.V. Ramachandran, P.D. Gagare, Inorg. Chem. 46 (2007) 7810–7817.
[3] A. Gutowska, L. Li, U. Shin, C.M. Wang, X.S. Li, J.C. Linehan, R.S. Smith, B.D. Kay, B. Schmid, W. Shaw, M. Gutowski, T. Autrey, Angew. Chem. Int. Ed. 44 (2005) pp.3578–3582.
[4] C.A. Jaska, K. Temple, A.J. Lough, I. Manners, J. Am. Chem. Soc. 125 (2003) 9424–9434.
[5] M.C. Denney, V. Pons, T.J. Hebden, D.M. Heinekey, K.I. Goldberg, J. Am. Chem. Soc. 128 (2006) 12048–12049.
[6] S.C. Amendola, S.L. Sharp-Goldman, M.S. Janjua, N.C. Spencer, M.T. Kelly, P.J. Petillo, M. Binder, Int. J. Hydrogen Energy 25 (2000) pp.969–975.
[7] R.J. Keaton, J.M. Blacquiere, R.T. Baker, J. Am. Chem. Soc. 129 (2007) 1844–1845.
[8] J.M. Yan, X.B. Zhang, S. Han, H. Shioyama, Q. Xu, Angew. Chem. Int. Ed. 47 (2008) 2287–2289.
[9] D.W. Himmelberger, C.W. Yoon, M.E. Bluhm, P.J. Carroll, L.G. Sneddon, J. Am. Chem. Soc. 131 (2009) 14101–14110.
[10] M.E. Bluhm, M.G. Bradley, R. Butterick III, U. Kusari, L.G. Sneddon, J. Am. Chem. Soc. 128 (2006) 7748–7749.
[11] D.W. Himmelberger, L.R. Alden, M.E. Bluhm, L.G. Sneddon, Inorg. Chem. 47 (2009) 9883–9889.
[12] F.H. Stephens, R.T. Baker, M.H. Matus, D.J. Grant, D.A. Dixon, Angew. Chem. 119 (2007) 760–763.
[13] D.J. Heldebrant, A. Karkamkar, N.J. Hess, M. Bowden, S. Rassat, F. Zheng, K. Rappe, T. Autrey, Chem. Mater. 20 (2008) 5332–5336.
[14] D. Neiner, A. Karkamkar, J.C. Linehan, B. Arey, T. Autrey, S.M. Kauzlarich, J. Phys. Chem. C 113 (2009) 1098–1103.
[15] Ned T. Stetson, in: DOE Annual Merit Review and Peer Evaluation Meeting, May 15, 2012. http://www.hydrogen.energy.gov/pdfs/review12/st000_stetson_2012_o.pdf.
[16] Y. Kim, H. Baek, J. Lee, S. Yeo, K. Kim, S. Hwang, B. Eun, S. Nam, T. Lim, C. Yoon, Phys. Chem. Chem. Phys. 15 (2013) 19584–19594.
[17] M. Diwan, H.T. Hwang, A. Al-Kukhun, A. Varma, AIChE J. 57 (2011) 259–264.
[18] Jamie Holladay Pacific Northwest National Laboratory Fuel Cell Seminar, Nov 7, 2012. http://www.fuelcellseminar.com/media/51173/mot32-2.pdf.
[19] Tessui Nakagawa, Biswajit Paik, Benjamin Davis, Troy Semelsberger, Tom Baker, Larry Sneddon, Annual Merit Review, May 17th Los Alamos National Laboratory LA-UR 12-20427, 2012. http://www.hydrogen.energy.gov/pdfs/review12/st040_davis_2012_o.pdf.
[20] K. Brooks, M. Devarakonda, S. Rassat, D. King, D. Herling, Int. J. Hydrogen Energy 37 (2012) 2779–2793.
[21] Troy A. Semelsberger, Ben L. Davis, Brian D. Rekken, Biswajit Paik, Jose I. Tafoya, in: Annual Merit Review Proceedings, May 13–17, 2013. http://www.hydrogen.energy.gov/pdfs/review13/st007_semelsberger_2013_o.pdf.
[22] Y. Kim, Y. Kim, Y. Kim, C.W. Yoon, S.-P. Yoon, S.W. Nam, S.A. Hong, J.H. Han, H.C. Ham, K. Kim, Korean Patent KR10-2012-0068200.
[23] Y. Kim, Y. Kim, S. Yeo, K. Kim, K.J.-E. Koh, J.-E. Seo, S.J. Shin, D.-K. Choi, C.W. Yoon, S.W. Nam, J. Power Sources 229 (2013) pp.170–178.
[24] AEROPAK, Standard Systems Specifications of Stacks, http://www.horizonfuelcell.com.
[25] C. Lee, S. Kim, D. Kim, J. Korean Soc. Propuls. Eng. 14 (2010) 65–70.
[26] D.W. Himmelberger, L.R. Alden, M.E. Bluhm, P.J. Carroll, L.G. Sneddon, Inorg. Chem. 48 (2009) 9883–9889.
[27] F.H. Stephens, V. Pons, R.T. Baker, Dalton Trans. (2007) 2613–2626.
[28] J.F. Kostka, R. Schellenberg, F. Baitalow, T. Smolinka, F. Mertens, Eur. J. Inorg. Chem. 2012 (2012) 49–54.
[29] R. Halseid, P.J.S. Vie, R. Tunold, J. Power Sources 154 (2006) 343–350.